JOURNAL OF MATERIALS SCIENCE 30 (1995) 3768–3772

Electrical properties of cement paste obtained from impedance spectroscopy

H. C. KIM, S. Y. KIM
Physics Department, Korea Advanced Institute of Science and Technology, 373-1, Kusong-dong Yusong-gu, Teajon, 305-701, Korea

S. S. YOON
Physics Department, Andong National University, 388, Songch'on-dong, Andong, Kyungbuk 760-749, Korea

The impedance spectra of hydrating Portland cement paste showed a small part of a large depressed arc and a single depressed arc at low- and high-frequency regions, respectively. A new equivalent circuit was proposed for hydrating cement paste, which consists of a serial combination of a resistor and a constant phase element (CPE) with a resistor in parallel for the bulk effects, and a parallel combination of a resistor and a CPE for the electrode effects. The microstructural evolution in hydrating cement paste was associated with the changes in the resistances, capacitance and the critical relaxation time.

1. Introduction

The impedance spectrum has been studied in an effort to separate the bulk cement electrical properties from measured electrical values and to represent microstructural changes of hydrating cement paste [1–4]. A single arc and a small part of a large arc of complex impedance plotted, respectively, in the high- and low-frequency ranges, are considered as evidence for Maxwell–Wagner effects in the bulk and an indicator of electrode effects, respectively. Several equivalent circuits [2–8] were proposed to account for the two observed arcs, such as an electrode R/C network and a constant phase element (CPE) in series with one or two bulk R/C networks and a bulk resistor [3]. The cut-off frequency at the intersection of the single arc with another large arc is envisaged to differentiate bulk effects from electrode effects, and the real impedance at that frequency is considered as the bulk ionic resistance of cement paste [1]. Each RC element of an equivalent circuit indicates microstructural evolution in hydrating cement paste [5–7, 9–11], such as C for the polarization change due to blocking of charges by cement grains or hydration products, and R the change of charge movement through water-filled capillary pores. However, data on the bulk electric parameters and relaxation time during hydration obtained from the analysis of the impedance spectra are scarce.

In the present work, a new equivalent circuit is proposed to characterize the whole impedance spectrum of hydrating cement paste and provide the physical meaning of each element. The microstructural evolution in hydrating cement paste was investigated with changes in resistance, capacitance and the critical relaxation time.

2. Experimental procedure

The specimen was prepared by mixing commercial ordinary Portland cement (OPC, Ssangyong Co., Korea) and deionized water. The mixed cement paste with a water/cement (W/C) ratio by weight of 0.4, was immediately poured into a dielectric mould of $16 \times 50 \times 75\ mm^3$, which consists of parallel electrodes of polished stainless steel at each side. The area, A, of the electrode and the distance, d, between the electrodes were $A = 1256\ mm^2$ and $d = 16\ mm$, respectively. The cement paste was hydrated under a constant temperature of $T = 30\,^{\circ}C$ in a temperature-controllable oven.

The complex impedances were measured in the frequency range 5 Hz–13 MHz with 20 readings per decade of frequency in logarithmic steps by using an HP-4192A impedance analyser controlled by a personal computer. Measurement was performed for 10 days from 10 min after mixing, with a reading cycle of every 10 min for 2 days, followed by 30 min thereafter.

The heat evolution rate during hydration was also measured by the conduction calorimetric method. The temperature of the hydrating cement paste was measured by the e.m.f. voltage of an embedded chromel–alumel thermocouple using a digital multimeter controlled by a personal computer.

3. Results and discussion

3.1. Frequency-dependent impedance of cement paste

The complex plots of real impedance, Z', and imaginary impedance, Z'', in Fig. 1 show an underdeveloped single arc in the high-frequency region, and a small part of a large arc in the low-frequency region,

0022–2461

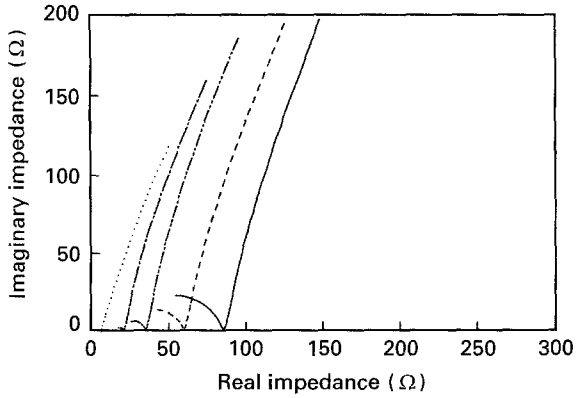

Figure 1 The complex plots of real impedance and imaginary impedance of hydrating cement paste. W/C = 0.4, T = 30 °C. (——) 10d, (– – –) 5d, (–·–·–) 2d, (–··–··–) 1d, (···) 10 min.

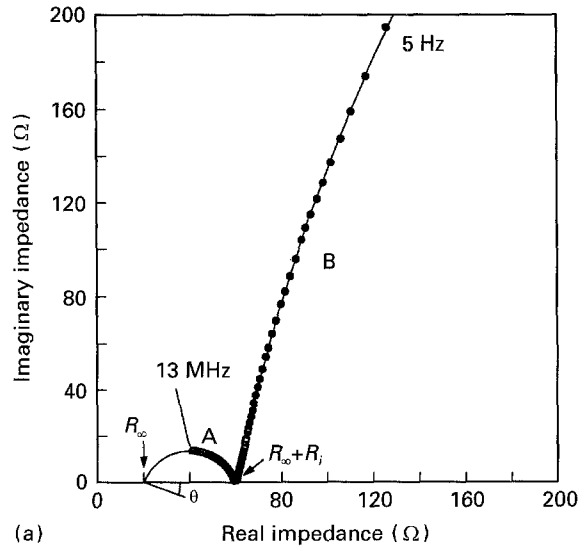

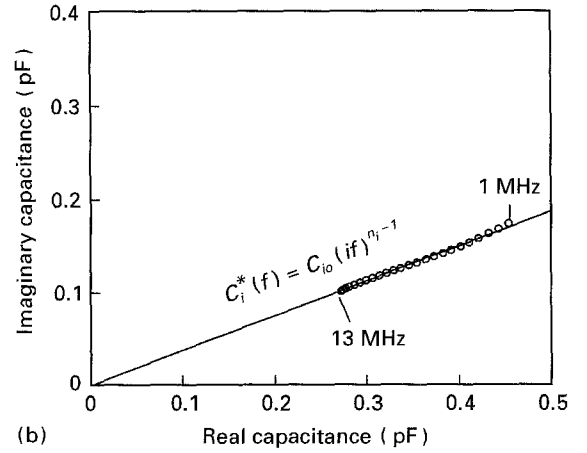

Figure 2 (a) Complex impedance of cement paste after 5 d hydration. (b) The complex plane plot of $C_i^*(f)$ (○) Experimental data, (——) fitted data with Equation 3.

similar to those of other workers [1–3, 5, 7, 11–13]. The small depressed arc of the bulk effect appeared after 2 days and the large depressed arc of the electrode effect appeared immediately after mixing of the cement paste with deionized water. The real impedance, Z', at the interception of the two arcs increased as hydration proceeded.

Fig. 2a is the impedance spectrum measured after 5 d hydration. The high-frequency arc, A, is a closed

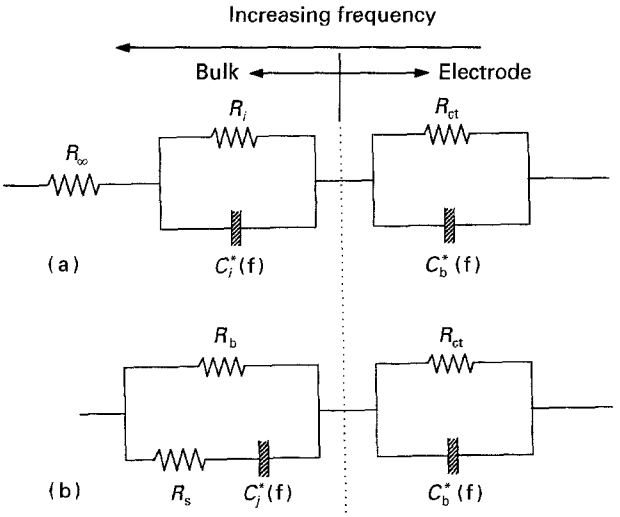

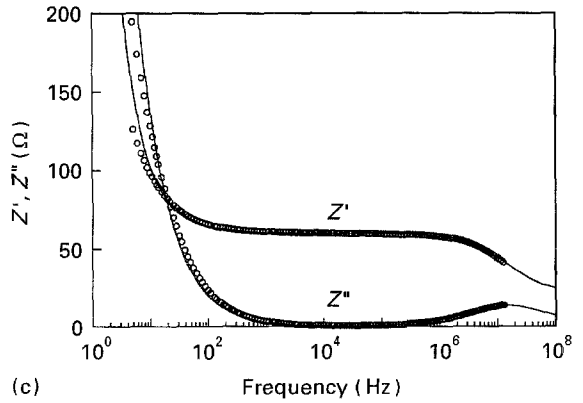

Figure 3 (a, b) Equivalent circuit models for cement paste/electrode system. (c) Complex impedance, $Z_t^*(f) = Z'(f) - iZ''(f)$, as a function of frequency for hydrating cement paste. (○) Experimental data, (——) fitted data with the equivalent circuit of (b).

arc with its centre lying below the real impedance axis, and R_∞ and $R_\infty + R_i$ correspond to abscissae intercepts of the arc, A, at high and low frequencies, respectively. Therefore, the single arc, A, is depicted with a parallel combination of R_i and an unknown $C_i^*(f)$ connected to R_∞ in series in Fig. 3a [14]. The resistances $R_\infty = 20.3\ \Omega$, $R_i = 39.4\ \Omega$ and the depressed angle $\theta = 20.5°$ were obtained by fitting the high-frequency arc, A, to the equation of a circle as follows

$$(Z' - Z_1)^2 + (Z'' - Z_2)^2 = r^2 \quad (1a)$$

$$R_\infty = Z_1 - (r^2 - Z_2^2)^{1/2} \quad (1b)$$

$$R_\infty + R_i = Z_1 + (r^2 - Z_2^2)^{1/2} \quad (1c)$$

$$\tan\theta = \frac{-Z_2}{Z_1 - R_\infty} \quad (1d)$$

where r and (Z_1, Z_2) are, respectively, the radius and centre of the circle in the real–imaginary impedance plane.

The resistances, R_∞ and R_i, can be subtracted numerically from the measured impedance, $Z^*(f) = Z'(f) - iZ''(f)$, at the frequency f by the relation

$$C_i^*(f) = \frac{1}{i2\pi f}\left[\frac{1}{Z^*(f) - R_\infty} - \frac{1}{R_i}\right] \quad (2)$$

The circle data of the remaining element $C_i^*(f)$ in Fig. 2b indicate a tilted straight line, corresponding to a constant phase type capacitance as follows

$$C_i^*(f) = C_{i0}(if)^{n_i - 1} \quad (3)$$

The parameters of $C_{i0} = 1.14 \times 10^{-8}$ F and $n_i = 0.77$ in Equation 3 were determined by the solid-line fitting of the experimental data in Fig. 2b.

By the same method as for the high-frequency arc, the low-frequency arc, B, in Fig. 2a is depicted with a parallel combination of the charge transfer resistance, R_{ct}, and the electrode barrier capacitance, $C_b^*(f) = C_{b0}(if)^{n_b - 1}$, as shown in Fig. 3a. The parameters $R_{ct} = 1760\,\Omega$, $C_{bo} = 1.49 \times 10^{-4}$ F and $n_b = 0.86$ were obtained from the best fitting of the low-frequency arc, B.

Fig. 3a is the complete circuit model obtained from the impedance spectrum of cement paste after 5 d hydration. Our equivalent circuit consists of a parallel combination of R_i and $C_i^*(f)$ with R_∞ in series to represent the bulk effects, and a parallel combination of R_{ct} and $C_b^*(f)$ to represent the electrode effects, similar to that of McCarter and Brousseau [2] except for the Warburg (or Faradic) impedance element and also similar to that of Ping Xie *et al.* [5].

An alternative equivalent circuit for Fig. 3a consists of a serial combination of a resistance, R_s, and $C_j^*(f)$ of the CPE with a resistance, R_b, in parallel as shown in Fig. 3b, which perfectly gives the same frequency response as that of Fig. 3a under the conditions

$$R_b = R_i + R_\infty \quad (4)$$

$$R_s = R_\infty\left(1 + \frac{R_\infty}{R_i}\right) \quad (5)$$

$$C_j^*(f) = \left(1 + \frac{R_\infty}{R_i}\right)^{-2} C_i^*(f) = C_{j0}(if)^{n_j - 1} \quad (6)$$

where $C_{j0} = [1 + (R_\infty/R_i)]^{-2} C_{i0}$ and $n_i = n_j$.

Under the assumption that the conduction processes in bulk cement paste are in parallel, we choose the equivalent circuit of Fig. 3b to describe the depressed arc in the complex impedance plane. Then, we obtain the values $R_b = 59.7\,\Omega$ and $R_s = 31.1\,\Omega$ using $R_i = 39.4\,\Omega$ and $R_\infty = 20.3\,\Omega$ for the cement paste hydrated for 5 d from Equations 4 and 5.

The total impedance, $Z_t(f)$, of the equivalent circuit given in Fig. 3b for the cement paste after 5 d hydration is given by the following equation.

$$Z_t(f) = \frac{R_s R_b}{R_s + R_b} + \frac{R_b^2/(R_s + R_b)}{1 + i2\pi f C_j^*(f)(R_s + R_b)} + \frac{R_{ct}}{1 + i2\pi f R_{ct} C_b^*(f)} \quad (7)$$

The solid line in Fig. 3c is the result of fitting $Z_t(f)$ with the parameters, $R_s = 31.1\,\Omega$, $R_b = 59.7\,\Omega$, $C_{j0} = 5.0 \times 10^{-12}$ F and $n_j = 0.77$ for $C_j^*(f)$, $R_{ct} = 1760\,\Omega$, $C_{b0} = 1.49 \times 10^{-4}$ F and $n_b = 0.86$ for $C_b^*(f)$, obtained from the analysis of the impedance spectrum for the cement paste after 5 d hydration. The correspondence between the measured impedance data of the circles and the total impedance, $Z_t(f)$, of the solid line is quite satisfactory, except for a slight deviation in the low-frequency region.

The physical process in the cement paste/electrode system is associated with the circuit elements in the equivalent circuit in the following manner. R_b, the corresponding bulk d.c. resistance in the cement paste, is associated with the presence of direct ion conduction through the long capillary pore channel making a conduction path between two electrodes. R_s is associated with the overall resistance of the water solution in blocked pores with a size distribution. The ions in blocked pores cannot contribute to the d.c. conductivity, but their contribution appears in the high-frequency dispersion region above 1 MHz, as represented by the second term of the right-hand side in Equation 7.

The representation of the high-frequency dispersion by $C_j^*(f)$ has been accepted as a universal dielectric response, because virtually all materials show a constant phase type of response [15, 16]. We ascribe the CPE response in the cement paste to a distribution of relaxation times caused by the motion of ions in the heterogeneous pore distribution [14]. Ions in the pore contribute to $C_j^*(f)$ of the CPE, by means of blocking by cement grains or by hydration products and conduction by charge transport through the pore network, respectively. The interfacial element, R_{ct}, is due to the charge transfer resistance at the electrodes. The barrier process $C_b^*(f)$ is encountered frequently at the solid material/electrode interface and has been considered as a diffusion-related process [17–21].

3.2. Change of electrical parameters given by impedance spectra during hydration

Fig. 4a shows the variation of the resistances R_s, R_b and R_{ct} obtained from impedance spectra during hardening of the cement paste. The sensitive change in the resistances, R_b and R_{ct}, from 2–10 d indicates continuous microstructural changes. The increase of the bulk d.c. resistance, R_b, suggests that the conduction path between two electrodes becomes more complex and truncated by the hydration products. The slight decrease of R_s indicates that the blocked pores are continuously produced by hydration products and contribute to the overall R_s, represented by parallel connection with R_b.

Fig. 4b shows the changes in R_b, R_{ct} and the heat evolution rate during the initial 2 d. R_s could not be determined during the first 2 d due to the underdeveloped high-frequency arc, which indicates that all ions in the cement paste can be transported through the whole material without blocking in the initial stage of hydration. As hydration proceeds, the blocked pores start to appear. Accordingly, R_s contributes to the high-frequency arc after 2 d as shown in Fig. 4a. The nearly parallel behaviour of R_b and R_{ct} with hydration time in Fig. 4a and b reflects that the charge transfer process is controlled by d.c. ionic conduction in the cement paste. As R_b increases, the number of ions reaching the electrode per unit time and per unit area decreases, hence R_{ct} increases.

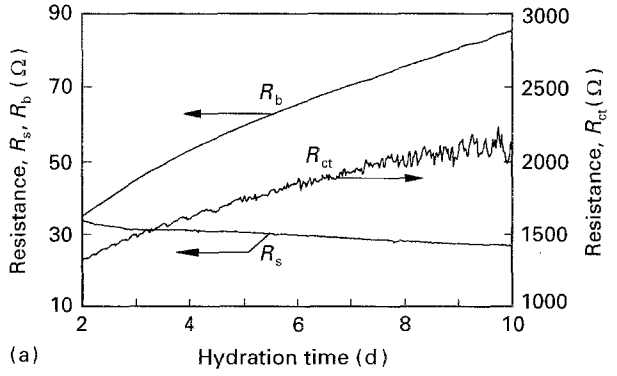

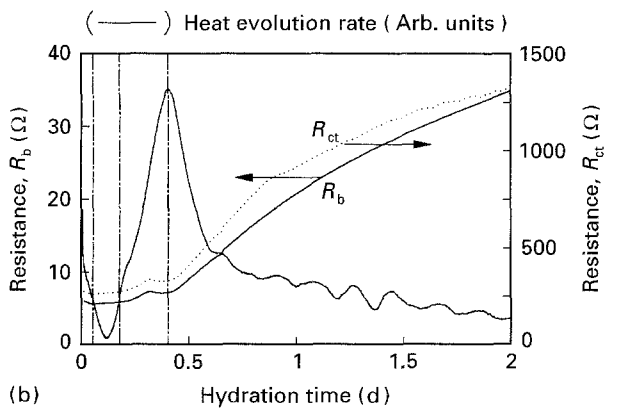

Figure 4 (a) Variation of the resistances R_s, R_b and R_{ct} during hardening of cement paste. (b) Variation of R_b, R_{ct} and heat evolution rate during the initial 2 d.

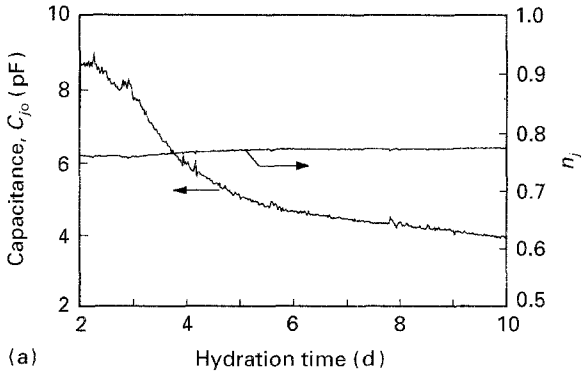

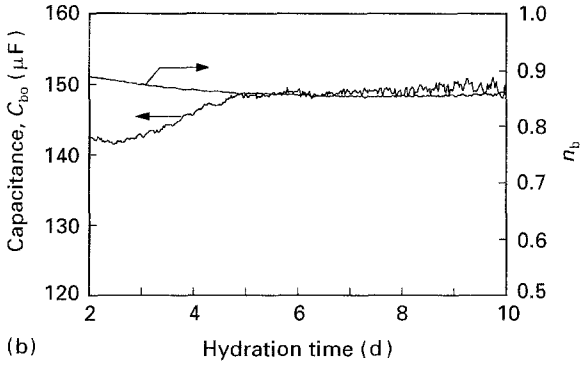

Figure 5 Variation of the coefficients, C_{j0} and n_j, for bulk CPE and the coefficients, C_{b0} and n_b, for electrode CPE during hydration of cement paste.

The variation of the two resistances, R_b and R_{ct}, during hydration in Fig. 4b shows four stages separated by vertical lines: a slow decrement, a plateau, a plateau after a small increment, and an increasing region. The first stage of slow decrement of resistance corresponds to the free-induction of the heat evolution rate and is due to the dissolution of ions from cement grains into the aqueous phase after mixing [22]. The second stage of the plateau region is attributed to the induction period, where the hydration reaction is very low. The third stage of an increase of the resistance during the acceleration period, where the heat evolution rate increases, is mainly caused by the decrease in the number of ions and ion mobility due to the formation of hydration products. The plateau resistance near the end of the accelerated period may reflect the competition between the resistance decrease due to the temperature rise [23] and the resistance increase due to the formation of hydration products. The last stage of increasing resistance corresponds to the deceleratory period characterized by the decrease of the heat evolution rate and is associated with a continuous decrease of mobility due to the solidification of the hydrating cement paste.

Fig. 5a and b show, respectively, the coefficients, C_{j0} and n_j, of $C_j^*(f)$ for the bulk CPE, and the coefficients, C_{b0} and n_b, of $C_b^*(f)$ for the electrode CPE. The powers n_j and n_b are nearly constant during hydration. The value of C_{j0} decreases continuously, while C_{b0} increases slightly for 5 d followed by saturation.

We consider the heterogeneous structure of the cement paste/electrode interface as the physical origin of $C_b^*(f)$ ($= C_{b0}(if)^{n_b-1}$), and it can be accounted for by Liu's or Kaplan–Gray's models for the fractal rough interface [24, 25], where they proposed an equivalent circuit for a rough interface between two materials of very different conductivities, e.g. an electrode and an electrolyte, represented by the CPE. The nearly constant n_b of $C_b^*(f)$ in Fig. 5 is attributable to the constancy of the heterogeneity of the electrode/cement paste, such as roughness during hydration. The increase of C_{b0} during hydration is due to the increase of the double-layer capacitance as the charge transfer resistance, R_{ct}, increases during hydration, as shown in Fig. 4.

In order to analyse the change of n_j and C_{j0} in Fig. 5a, we use the following alternative representation for the impedance of the bulk part in the equivalent circuit of Fig. 3b.

$$Z^*(f) = R_\infty + \frac{R_b - R_\infty}{1 + (i2\pi f\tau_0)^{1-\alpha}} \quad (8)$$

$$\tau_0 = [C_{j0}(R_s + R_b)]^{1/n_j}(2\pi)^{(1/n_j)-1} \quad (9)$$

where $R_\infty = R_bR_s/(R_b + R_s)$ and $\alpha = 1 - n_j$. The relaxation time τ is not single-valued but is distributed continuously or discretely around the critical relaxation time τ_0. The values of α are related to the width of the relaxation time distribution [14, 26], which is caused by the distribution of pore sizes and many kinds of ions in the hydrating cement paste. The change of τ_0 and α transformed from R_s, R_b, C_{j0} and n_j, is shown in Fig. 6.

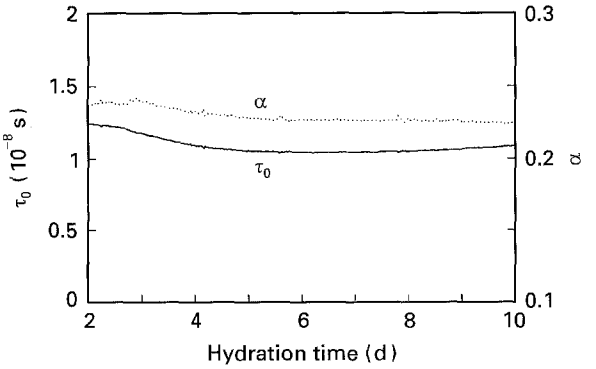

Figure 6 Variation of τ_0 and α calculated from electrical parameters R_s, R_b, C_{j0} and n_j during hydration of cement paste.

The slight decrease of α from 2–10 d in Fig. 6 is attributable to the decreased width of the relaxation time distribution. This indicates that the distribution of pores becomes simpler as the hydration products fill up the space of the pores, although the change is small due to the slow rate of hydration.

The critical relaxation time, τ_0, in Fig. 6 changes slowly during hydration in spite of the increase of resistance, R_b. This indicates that the decrease of the capacitance, C_{j0}, is accompanied by hydration in the cement paste, as shown in Fig. 5a, because the changes of R_s and n_j in Equation 9 are small during hydration. This result is consistent with the constancy of the angular frequency, ω_0, associated with the peak of the circular arc obtained from two-dimensional models of cement paste by Coverdale *et al.* [27], where they showed that the change of the microstructure in cement paste did not influence the angular frequency, $\omega_0 = 1/\tau_0$.

4. Conclusion

The impedance spectrum of hydrating cement paste was represented by an equivalent circuit involving a serial combination of R_s and $C_j^*(f)$ with R_b in parallel for bulk effects and a parallel combination of R_{ct} and $C_b^*(f)$ for the interface effects. The increase of bulk d.c. resistance, R_b, during hydration indicates that the conduction path between two electrodes becomes complex and truncated by the hydration products. The decrease of the overall resistance, R_s, of water solution in blocked pores during hydration, indicates that the blocked pores are continuously produced by hydration products. $C_j^*(f)$ of the CPE in the bulk is due to blocking of ions by cement grains or by hydration products in the distribution of heterogeneous pores. The impedance, $Z^*(f)$, of the bulk part in the equivalent circuit represents the cement paste as a heterogeneous material having a relaxation time distribution due to various distributions of pore size and many kinds of ions in the hydrating cement paste. The R_{ct} and $C_b^*(f)$ represent, respectively, the charge transfer resistance and barrier process at the cement paste/electrode interface. The four-stage variation of the heat evolution rate was explained in terms of the changes of R_{ct} and R_b, indicating that the resistance of the cement paste is closely related to the microstructural evolution in the hydrating cement paste. The critical relaxation time of a bulk depressed arc had a nearly constant value in spite of microstructural changes in the hydrating cement paste, indicating that the increase of bulk d.c. resistance during hydration accompanies the decrease of bulk capacitance.

References

1. W. J. McCARTER, S. GARVIN and N. BOUZID, *J. Mater. Sci. Lett.* **7** (1988) 1056.
2. W. J. McCARTER and R. BROUSSEAU, *Cem. Concr. Res.* **20** (1990) 891.
3. C. A. SCUDERI, T. O. MASON and H. M. JENNINGS, *J. Mater. Sci.* **26** (1991) 349.
4. K. BRANTERVIK and G. A. NIKLASSON, *Cem. Concr. Res.* **21** (1991) 496.
5. PING GU, PING XIE, J. J. BEAUDOIN and R. BROUSSEAU, *ibid.* **22** (1992) 833.
6. PING XIE, PING GU, ZHONGZI XU and J. J. BEAUDOIN, *ibid.* **23** (1993) 359.
7. PING GU, PING XIE, J. J. BEAUDOIN and R. BROUSSEAU, *ibid* **23** (1993) 157.
8. PING GU, ZHONGZI XU, PING XIE and J. J. BEAUDOIN, *ibid* **23** (1993) 675.
9. *Idem, ibid.* **23** (1993) 531.
10. ZHONGZI XU, PING GU, PING XIE and J. J. BEAUDOIN, *ibid.* **23** (1993) 1007.
11. *Idem, ibid.* **23** (1993) 853.
12. PING GU, PING XIE and J. J. BEAUDOIN, *ibid.* **23** (1993) 581.
13. B. J. CHRISTENSEN, T. O. MASON and H. M. JENNINGS, *J. Am. Ceram. Soc.* **75** (1992) 939.
14. I. D. RAISTRICK, J. R. MACDONALD and D. R. FRANCESCHETTI, in "Impedance Spectroscopy", edited by J. R. Macdonald (Wiley, New York, 1987) Ch. 2.
15. A. K. JONSCHER, *Nature* **267** (1977) 673.
16. R. M. HILL, *ibid.* **275** (1978) 96.
17. P. H. BOTTELBERGHS, in "Solid Electrolytes", edited by P. Hagenuller and W. Van Gool (Academic, New York, 1978) Ch. 10.
18. P. H. BOTTELBERGHS and G. H. J. BROERS, *J. Electroanal. Chem.* **67** (1976) 155.
19. I. R. RAISTRICK, C. HO and R. A. HUGGINS, *J. Electrochem. Soc.* **123** (1976) 1469.
20. J. R. MACDONALD, *Solid State Ionics* **13** (1984) 147.
21. L. A. DISSADO and R. M. HILL, *J. Chem. Soc. Farad. Trans. 2* **80** (1984) 291.
22. J. F. YOUNG, H. S. TONG and P. L. BERGER, *J. Am. Ceram. Soc.* **60** (1977) 193.
23. W. J. McCARTER and A. B. AFSHAR, *J. Mater. Sci.* **23** (1988) 488.
24. S. H. LIU, *Phys. Rev. Lett.* **55** (1985) 529.
25. T. KAPLAN and L. J. GRAY, *Phys. Rev. B* **32** (1985) 7360.
26. C. J. F. BOTTCHER and P. BORDEWIJK, "Theory of Electric Polarization (II)" (New York, 1978) Ch. 9.
27. R. T. COVERDALE, B. J. CHRISTENSEN, T. O. MASON and H. M. JENNINGS, *J. Mater. Sci.* **29** (1994) 4984.

Received 18 November
and accepted 13 December 1994